Thermochimica Acta, 149 (1989) 71–86
Elsevier Science Publishers B.V., Amsterdam – Printed in The Netherlands

THE PbO_2–PbO–B_2O_3 SYSTEM IN AIR

Y.M. KASSEM, A.N. MAHDY and M.F. ABADIR

Chemical Engineering Department, College of Engineering, Cairo University, Giza (Egypt)

(Received 17 October 1988)

ABSTRACT

A ternary isobaric diagram has been drawn for the PbO_2–PbO–B_2O_3 system in air. The occurrence of the compounds $PbO \cdot 2B_2O_3$, $PbO \cdot B_2O_3$ (s.s.), $2PbO \cdot B_2O_3$ (s.s.) and $4PbO \cdot B_2O_3$ has been confirmed, and their stability regions fixed. PbO has also been found to exist in this system as a solid solution. The presence of B_2O_3 destabilizes Pb_3O_4, causing it to dissociate to PbO at 490 °C, rather that at 560 °C as for the pure oxide.

INTRODUCTION

Lead borate glasses have long been used, alone and with other oxides, for their exceptional optical properties. In recent years, however, new applications have appeared, which have necessitated a more detailed investigation of the relevant phase diagram.

Table 1 shows some of the most important uses of lead borate glasses.

Phase equilibrium studies in this area have not considered the polyvalent nature of Pb. In the present work this was taken into consideration, and consequently the diagram for the system PbO_2–PbO–B_2O_3 was studied.

REVIEW OF PREVIOUS WORK

Lead borates

Various studies of lead borates have been reported. Table 2 summarizes the available data.

The binary system Pb–O

Abadir et al. [18] have established this system, at between 0.21 and 1.0 atm. O_2.

0040-6031/89/$03.50

TABLE 1

Applications of $PbO-B_2O_3$ glasses

No.	Scope of use	Specific uses	Composition	References
1	Optical properties	Eye glasses with high *n*	$PbO-B_2O_3$	1
		Radiation absorption (X- and γ-rays)	$PbO-B_2O_3$	2
2	Electrical properties	Dielectricity	$PbO-B_2O_3-Fe_2O_2$	3
			$PbO-B_2O_3-SiO_2$	4
		High frequency capacitors	$PbO-B_2O_3-TiO_2$	5
		Thick film resistors	$PbO-B_2O_3-Bi_2O_3$	6
3	Decoration	Glass frit	$PbO-B_2O_3-Na_2O$	7
		Enamel on Al	$PbO-B_2O_3$	8
4	Joint sealing		$PbO-B_2O_3$	9
			$PbO-B_2O_3-ZnO$	10
			$PbO-B_2O_3-V_2O_3$	11
5	Piezo-electricity		$PbO-B_2O_3-V_2O_5$	12

TABLE 2

Previous studies of lead borates

Compound	$PbO:B_2O_3$ (molar)	Notes	References
$PbO \cdot 2B_2O_3$	1:2	Formed by s.s. reaction of $Pb(NO_3)_2$ and H_3BO_3	13
		Melts congruently at 768 °C	14, 15, 16, 17
$PbO \cdot B_2O_3$	1:1	Allotropic transition β to α form at 460 °C	13
$5PbO \cdot 4B_2O_3$	5:4	Melts incongruently at 548 °C	14, 16, 17
$9PbO \cdot 8B_2O_3$	9:8	Metastable	13
$2PbO \cdot B_2O_3$	2:1	Occurs in two forms	14, 15
		(Transition at 473 °C)	16
		Melts incongruently at 497 °C	17
$4PbO \cdot B_2O_3$	4:1	Occurs in two forms (Transition at 552 °C)	15, 17
		Melts congruently at 565 °C	14

The system $PbO-B_2O_3$

The first attempt to investigate the phase equilibrium for this system was made by Geller and Bunting [14], who presented the phase diagram in Fig. 1. In this diagram four intermediate compounds are formed: $PbO \cdot 2B_2O_3$, which melts congruently at 768 °C; $5PbO \cdot 4B_2O_3$, which melts incongruently at 548 °C; $2PbO \cdot B_2O_3$, which occurs in two allotropic modifica-

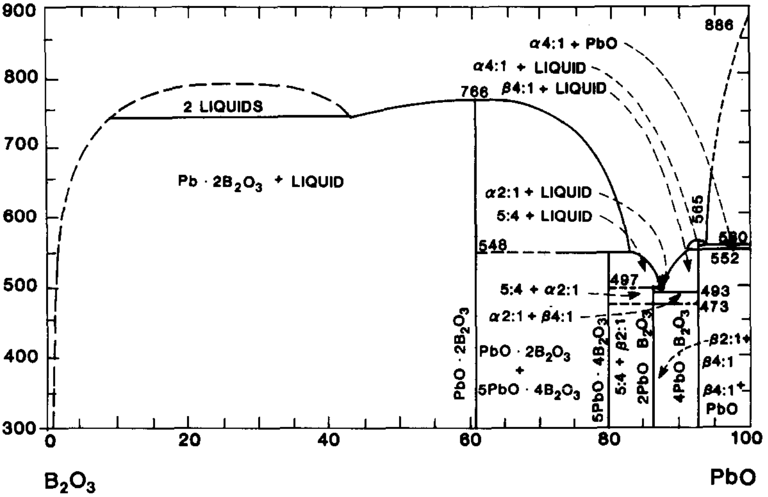

Fig. 1. The system $PbO-B_2O_3$, after Geller and Bunting [14].

tions with a transition temperature of 473° C, and is shown on the diagram to melt incongruently at 497° C; and $4PbO \cdot B_2O_3$, which occurs in two allotropic forms with a transition temperature of 552° C, and is shown on the diagram to melt congruently at 565° C.

The diagram also shows a region of liquid immiscibility, occurring on the high B_2O_3 side. This has been confirmed by Liedberg et al. [19], who proposed an immiscibility gap reaching as far as 45% PbO by weight (see Fig. 2). However, the diagram in Fig. 1 suffers from a number of defects. First, the eutectic formed between $PbO \cdot 2B_2O_3$ does not appear on the figure. Also, the region containing $PbO \cdot 2B_2O_3$ and low borax liquid in equilibrium should have been delimited by a horizontal line at the monotectic temperature. The same remarks hold for the diagram of Liedberg et al. [19].

More recently, Bauer and Plotcher [13] have published a diagram covering the compositions $(PbO/B_2O_3) = 1/2$ to $5/4$ (molar) showing three intermediate compounds of closely similar composition. Two of these were reported to be unstable (1 : 1, 9 : 8), and the third to be stable (5 : 4).

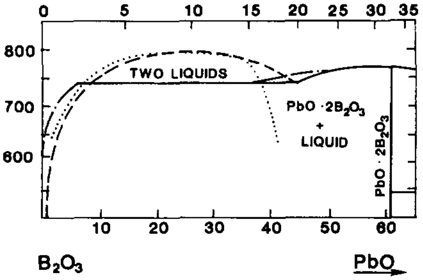

Fig. 2. The immiscibility region for the system $PbO-B_2O_3$ [19].

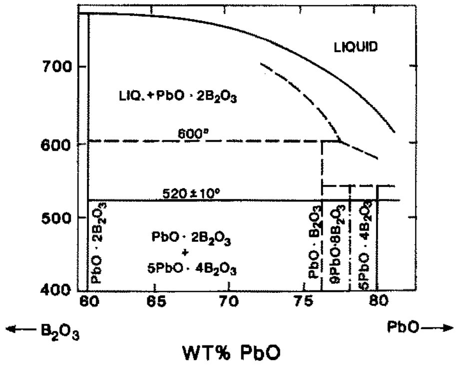

Fig. 3. The system $PbO \cdot 2B_2O_3$–$5PbO \cdot 4B_2O_3$ (revised), showing three metastable compounds [13].

In Fig. 3 the dotted area shows metastable lines. However, it is not likely that the three aforementioned compounds have the same melting point, as this figure would suggest. In view of the similar X-ray patterns of the compounds $PbO \cdot B_2O_3$ [20] and $5PbO \cdot 4B_2O_3$ [21], it would seem that these two compounds are members of a solid solution, particularly given the slight shift observed in *d*-spacings [22] (see Table 3).

TABLE 3

X-ray data for $PbO \cdot B_2O_3$ and $5PbO \cdot 4B_2O_3$

$PbO \cdot B_2O_3$ [20]		$5PbO \cdot 4B_2O_3$ [21]	
d (Å)	I/I_0	*d* (Å)	I/I_0
3.59	80	5.89	100
3.34	80	3.39	100
3.12	100	3.15	100
3.07	60	3.07	100
2.94	40	2.96	50
2.86	80	2.83	20
2.71	40	2.71	40
2.28	60	2.28	20
2.25	40	–	–
2.07	20	2.07	80
–	–	2.01	60
–	–	1.94	80
1.92	20	1.91	20
1.85	20	1.84	20
1.80	80	1.81	20
1.77	60	1.78	20
1.74	20	1.74	20
1.71	80	1.70	60
1.66	60	1.66	60
1.65	80	1.64	40

It should be noted that all previous investigations have used PbO as the original source of lead, i.e. the polyvalent nature of lead has been ignored. This is one reason why the present investigation was begun using the highest possible valency of lead (PbO_2).

EXPERIMENTAL

Raw materials

The lead oxide used was PbO_2 (A.R.; VEB Laborchemie Apolda, East Germany), containing a maximum of 0.7% impurities. This was dried at 120 °C prior to use.

The source of B_2O_3 was boric acid (H_3BO_3) supplied by the El-Nasr Pharmachemical Co. (Abu-Zaabal), containing a maximum of 0.5% impurities.

The thermal decomposition of boric acid has been investigated by many authors (see e.g. ref. 13). It is agreed that HBO_2 is formed at about 130 °C, this is followed by two allotropic transitions, ultimately reaching B_2O_3 at

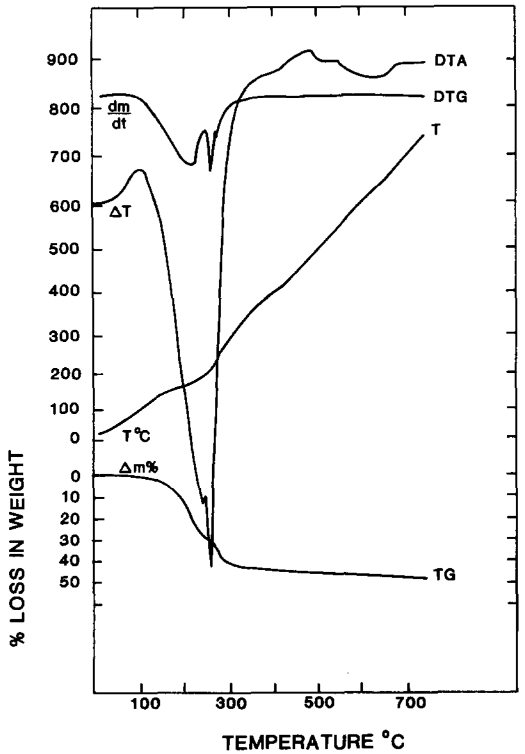

Fig. 4. Thermal analysis of boric acid (H_3BO_3) with a heating rate of 10 °C min^{-1}.

about 240 °C. This is confirmed by the combined TG and DTA shown in Fig. 4, as prepared by the present authors. It can be seen that loss of H_2O proceeds in two stages, ending at about 280 °C at a heating rate of 10 °C min^{-1}. This temperature coincides with the transition from PbO_2 to PbO_x ($x = 1.57$), so it can be assumed that all equilibrium mixtures of PbO_2 and H_3BO_3 at about 280 °C consist of B_2O_3 and PbO_x.

Preparation of mixtures

The mixtures were prepared by weighing out the appropriate amounts of PbO_2 and H_3BO_3 and mixing these, dry, in an agate mortar. The mixtures were then hung in the thermobalance and the temperature raised to 280 °C until constant weight was obtained. The various mixtures on the phase equilibrium diagram B_2O_3–PbO_2–PbO would then lie on the B_2O_3–$PbO_{1.57}$ conjugation line.

RESULTS AND DISCUSSION

Dissociation curves in air

The dissociation curves of mixtures initially containing 20, 30, 40, 50, 60, 70, 80, 86 and 90% PbO_2 were investigated. The various features observed in these curves are represented in Figs. 5, 6 and 7, which show the behaviour of mixtures of compositions 20, 40, 60, 70 and 90% PbO_2, respectively, when heated in the thermobalance in air.

These dissociation curves were used to construct the isobaric ternary diagram shown in Fig. 8. The thin horizontal lines represent the dissociation

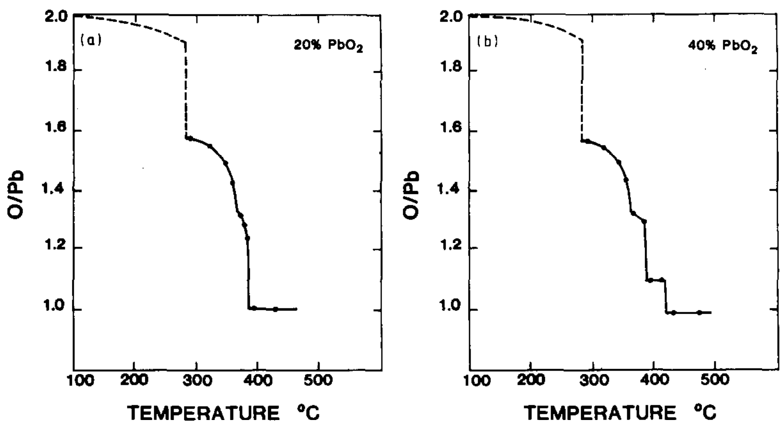

Fig. 5. Dissociation curves: a, the mixture with $PbO_2:B_2O_3 = 1:4$ (molar) in air; b, the mixture with $PbO_2:B_2O_3 = 2:3$ (molar) in air.

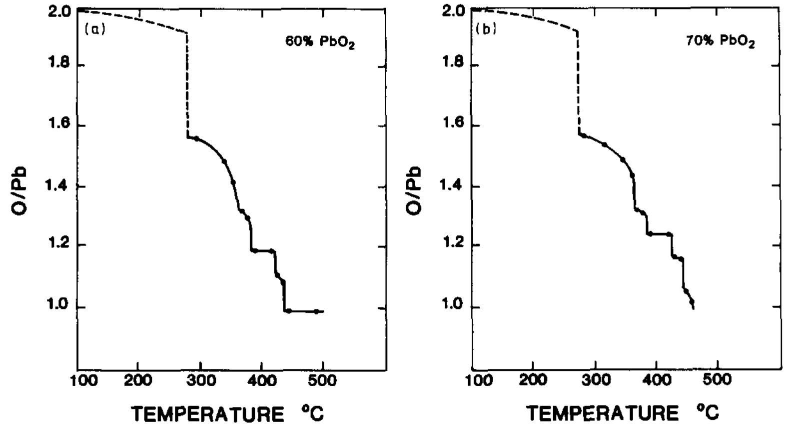

Fig. 6. Dissociation curves: a, the mixture with $PbO_2:B_2O_3 = 3:2$ (molar) in air; b, the mixture with $PbO_2:B_2O_3 = 7:3$ (molar) in air.

paths along which oxidation–reduction reactions occur. On these dissociation paths, the compositions reached on the dissociation curves at selected temperatures were calculated and plotted. The isothermal triangles obtained on this ternary diagram represent monovariant situations, appearing on the dissociation curves as vertical steps and implying the existence of three condensed phases as well as the gas phase. Straight lines connecting B_2O_3 with the lead oxides represent tie lines (two condensed phases and the gas phase). The compositions lying on these tie lines represent compositions on curved paths of the dissociation curves (i.e. bivariant situations). In all the mixtures a progressive oxygen loss is observed, from 280 °C to 364 °C, whereby oxygen is lost progressively to give B_2O_3 and $PbO_{1.41}$; this latter phase dissociates isothermally to Pb_3O_4 at 364 °C. Above 364 °C a slight

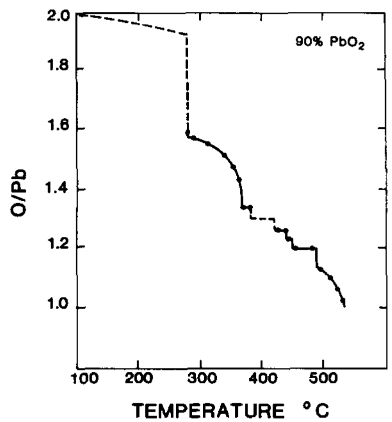

Fig. 7. Dissociation curve of the mixture with $PbO_2:B_2O_3 = 9:1$ (molar) in air.

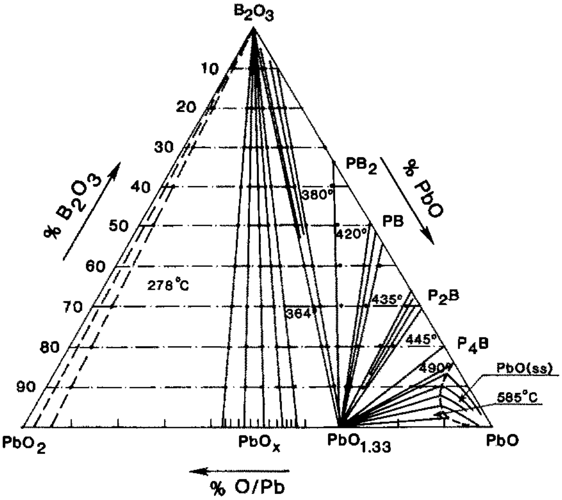

Fig. 8. Ternary isobar for the system PbO_2–PbO–B_2O_3 in air (molar basis).

oxygen loss occurs with the formation of B_2O_3 solid solution. At 380 °C an isothermal loss occurs, owing to the formation of $PbO \cdot 2B_2O_3$ according to the reaction

$$Pb_3O_4 + 6B_2O_3 \rightarrow 3(PbO \cdot 2B_2O_3) + \tfrac{1}{2}O_2 \qquad (1)$$

and in mixtures initially containing more than 67% B_2O_3 the O/Pb ratio drops from approximately 1.3 to 1.0. At temperatures above 380 °C different patterns of behaviour were observed, the characteristics of which are represented on the various dissociation curves.

Mixtures initially containing more than 67% B_2O_3

The behaviour of these mixtures can be represented by that of the mixture initially containing 20% PbO_2 (Fig. 5a). At the end of the step at 380 °C these mixtures consist of B_2O_3 and $PbO \cdot 2B_2O_3$ and the weight remains constant up to 760 °C, after which the quenched sample is found to be completely molten.

To assist the interpretation of the dissociation curves in this region a combined TG, DTA and DTG study was performed, using an alumina crucible and a heating rate of 10 °C min^{-1}, on a sample having the initial composition 30% PbO_2 (molar) (see Fig. 9). The peaks on the DTA curve (all endothermic) were numbered from 1 to 7, as were the corresponding points on the TG and DTG curves. Table 4 summarizes the results obtained. It should be noted that the temperatures obtained using the derivatograph are higher than the corresponding equilibrium temperatures. This is because of the relatively high rate of heating with the derivatograph (10 °C min^{-1}). It is also worth noting that the eutectic formed between B_2O_3 and $PbO \cdot 2B_2O_3$ above 600 °C has not been reported previously.

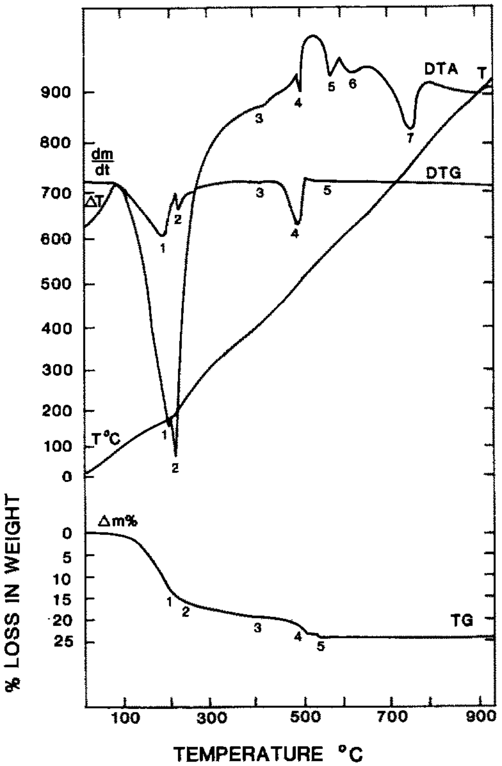

Fig. 9. Thermal analysis of $3PbO_2 \cdot 7B_2O_3$ with a heating rate of 10 °C min^{-1}.

It is unlikely that this temperature is that of the monotectic associated with the miscibility gap, since this gap has been reported by many authors to be above 700 °C [14].

TABLE 4

Combined thermal analysis of a mixture containing $3PbO_2 : 7B_2O_3$ (molar)

Peak number	Type	Temperature (°C)	Change in weight	Interpretation
1	endo	110–180	yes	H_3BO_3 to HBO_2
2	endo	180–340	yes	HBO_2 to $\frac{1}{2}B_2O_3$
3	endo	390–420	yes	Formation of PbO_x and loss of oxygen to Pb_3O_4
4	endo	460–510	yes	formation of $2PbO \cdot B_2O_3$
5	endo	570–600	very slight	Probably slight non-stoichiometry
6	endo	600–670	no	Formation of eutectic between B_2O_3 and $PbO \cdot 2B_2O_3$
7	endo	680–790	no	Final melting

Mixtures initially containing between 30 and 67% B_2O_3

These mixtures are typified by the mixture initially containing 40% PbO_2, the dissociation curve for which is shown in Fig. 5b. As is the case for mixtures containing more than 67% B_2O_3, at 364 °C this mixture consists of B_2O_3 and Pb_3O_4. At 380 °C, after a slight loss of oxygen, an isothermal step occurs as a result of reaction (1), giving off $PbO \cdot 2B_2O_3$ and Pb_3O_4. The weight then remains constant up to 420 °C, when another isothermal step takes place accompanied by the O/Pb ratio reaching unity. This second step is due to the reaction

$$3(PbO \cdot 2B_2O_3) + Pb_3O_4 \rightarrow 6(PbO \cdot B_2O_3) + \tfrac{1}{2}O_2 \qquad (2)$$

No further weight loss is observed, and at 650 °C the sample consists of a glassy liquid.

Mixtures initially containing between 33 and 50% B_2O_3

Mixtures of this composition are represented by the mixture containing 40% B_2O_3 (60% PbO_2), the dissociation curve for which is shown in Fig. 6a. In view of this dissociation curve and the ternary air isobar (Fig. 8), the following interpretations can be given.

Mixtures in this region at 364 °C consist of Pb_3O_4 and B_2O_3. A progressive loss in weight is observed up to 380 °C. Reaction (1) occurs to give Pb_3O_4 and $PbO \cdot 2B_2O_3$. The weight then remains constant up to 420 °C where reaction (2) occurs, accompanied by an isothermal loss in weight, to give $PbO \cdot B_2O_3$ and Pb_3O_4. Then a slight weight loss occurs up to 435 °C as Pb_3O_4 and $PbO \cdot B_2O_3$ (s.s.) coexist in equilibrium.

The O/Pb ratio reached just below 435 °C will depend on the original composition of the mixture. At 435 °C an isothermal loss in weight occurs, reducing the O/Pb ratio to unity. This is due to the reaction

$$3(PbO \cdot B_2O_3) + Pb_3O_4 \rightarrow 3(PbO \cdot B_2O_3) + \tfrac{1}{2}O_2 \qquad (3)$$

No further weight change has been detected. The sample containing 40% B_2O_3 was found to be completely molten at 660 °C. That reaction (3) occurs in association with the formation of $2PbO \cdot B_2O_3$ has been proven through X-ray analysis of a sample of initial composition 33% B_2O_3, after quenching at 450 °C. The lines obtained consisted exclusively of the compound $2PbO \cdot B_2O_3$, as compared with the ASTM cards of that compound [23].

Mixtures initially containing between 20 and 33% B_2O_3

The behaviour of these mixtures can be represented by the dissociation curve shown in Fig. 6b, corresponding to a mixture initially containing 30% B_2O_3 (70% PbO_2).

All these mixtures undergo reactions (1), (2) and (3) as described previously. Just below 435 °C the mixture of initial composition 70% PbO_2 consists of $PbO \cdot B_2O_3$ and Pb_3O_4. The isothermal step accompanying reac-

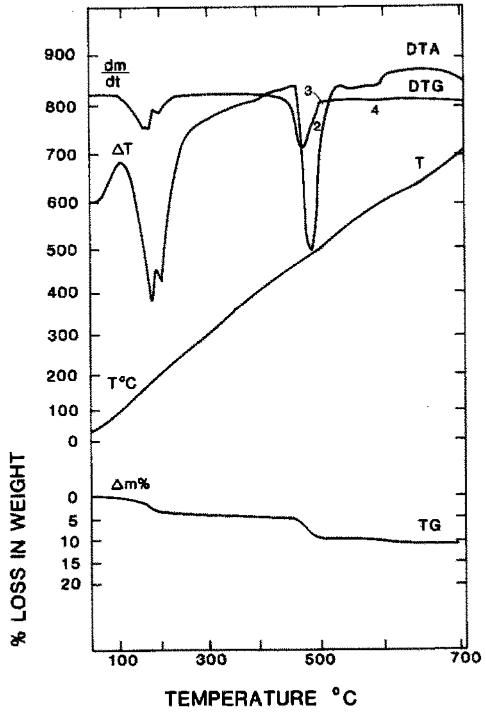

Fig. 10. Thermal analysis of $4PbO_2 \cdot B_2O_3$ with a heating rate of 10 °C min^{-1}.

tion (3) does not reduce the O/Pb ratio to unity but rather to 1.05. After this there occurs, progressively, a slight decrease in weight, implying that $2PbO \cdot B_2O_3$ is slightly non-stoichiometric. At 445 °C the O/Pb ratio reaches 1 and no further weight changes are detected. The border composition containing 20% B_2O_3 (80% PbO_2) behaves in the same way except that at 445 °C the O/Pb ratio is 1.13, reaching unity after an isothermal step which can be seen (Fig. 8) to correspond to the reaction

$$2Pb_3O_4 + 3(2PbO \cdot B_2O_3) \rightarrow 3(4PbO \cdot B_2O_3) + O_2 \qquad (4)$$

This particular composition (20% B_2O_3) has been studied on the derivatograph (see Fig. 10). After an initial loss in weight terminating at 240 °C the weight remains constant up to 400 °C, as can be seen from the TG curve. Oxygen is then lost in at least four stages, which we have numbered 1 to 4. Reaction 1 consists of the formation of Pb_3O_4 and $PbO \cdot 2B_2O_3$. Reactions 2 and 3 are probably associated with the formation of $PbO \cdot B_2O_3$ and $2PbO \cdot B_2O_3$, while reaction 4, corresponding to an O/Pb ratio of unity, indicates the formation of $4PbO \cdot B_2O_3$. The O/Pb ratios as calculated from the TG trace are: point (1), 1.33; point (2), 1.18; point (3), 1.1; and point (4), 1.0. The corresponding ratios as calculated from the determination of the isothermal steps of 20% B_2O_3 mixtures on the thermobalance are: point (1), 1.32; point (2), 1.22; point (3), 1.12; and point (4), 1.0.

Mixtures initially containing less than 20% B_2O_3

The dissociation curve for a mixture initially containing 10% B_2O_3 (90% PbO_2) is shown in Fig. 7. Owing to the high PbO_2 content, it was difficult to follow up isothermal steps from 380–435 ° C. However, an isothermal step is evident at 445 ° C, associated with the formation of $4PbO \cdot B_2O_3$. The weight then remains constant up to about 490 ° C where a gradual weight loss occurs, shifting the O/Pb ratio down to unity. This is due to the final decomposition of Pb_3O_4 to PbO. Although this decomposition takes place for pure oxide at 560 ° C, it has also been observed to occur at a lower temperature, presumably as a result of the formation of a solid solution zone on the high PbO side, as shown in Fig. 8.

The ternary isobaric section in air

Figure 8 shows the ternary isobaric section in air, constructed by projecting the compositions at the beginning and the end of each step of the dissociation curves on horizontal decomposition lines at constant B_2O_3/PbO ratio (molar). As previously stated, isothermal steps correspond to tie triangles on the ternary diagram, where three condensed phases and oxygen coexist at equilibrium. Seven of these invariant situations appear on the diagram. A tie triangle joining B_2O_3, PbO_x ($x = 1.57$) and PbO_2 (s.s.) should have occurred at about 278 ° C, which is the temperature at which PbO_2 (s.s.) decomposes to PbO_x in the pure state. However, since in this work the original source of B_2O_3 was boric acid which lost water within the same temperature range, no experimental points in this region are available, and the B_2O_3–PbO_2 (s.s.) tie lines are shown dotted on the diagram.

(i) At 364 ° C the condensed phases B_2O_3, PbO_x ($x = 1.41$) and Pb_3O_4 coexist in equilibrium with oxygen.

(ii) At 380 ° C B_2O_3 (s.s.), Pb_3O_4 and $PbO \cdot 2B_2O_3$ coexist in equilibrium with oxygen.

(iii) At 420 ° C Pb_3O_4, $PbO \cdot 2B_2O_3$ and $PbO \cdot B_2O_3$ (s.s.) coexist in equilibrium with oxygen.

(iv) At 435 ° C $PbO \cdot B_2O_3$ (s.s.), $2PbO \cdot B_2O_3$ (s.s.) and Pb_3O_4 coexist in equilibrium with oxygen.

(v) At 445 ° C $2PbO \cdot B_2O_3$ (s.s.), $4PbO \cdot B_2O_3$ and Pb_3O_4 coexist in equilibrium with oxygen.

(vi) At 490 ° C $4PbO \cdot B_2O_3$, PbO (s.s.) and Pb_3O_4 coexist in equilibrium with oxygen.

On the ternary diagram there appear five monovariant situations where two condensed phases coexist in equilibrium with oxygen. This is usually the case when at least one of these phases is a solid solution. The tie lines joining the two condensed phases show a progressive increase in temperature corresponding to those regions on the dissociation curves where oxygen is lost progressively.

(a) B_2O_3 coexists in equilibrium with PbO_2 (s.s.) and O_2 at temperatures ranging from about 100 to 278 ° C.

(b) PbO_x (s.s.) coexists in equilibrium with B_2O_3 and O_2 at temperatures ranging from 278 to 364 ° C.

(c) Between 364 and 380 ° C B_2O_3 takes some Pb_3O_4 in solid solution; hence in this temperature range B_2O_3 (s.s.) will coexist in equilibrium with Pb_3O_4 and O_2.

(d) The compound $PbO \cdot B_2O_3$ was found to be non-stoichiometric, as evidenced by its presence over a small range of compositions where PbO/B_2O_3 is slightly higher than unity. Consequently it will coexist in equilibrium with Pb_3O_4 and O_2 at temperatures ranging from 420 to 435 ° C.

(e) Similarly, the compound $2PbO \cdot B_2O_3$ was found to be non-stoichiometric and coexists in equilibrium with Pb_3O_4 and O_2 at temperatures ranging from 435 to 445 ° C.

For compositions extremely rich in PbO_2, the last isothermal step leading to the formation of PbO occurs at 490 ° C. This suggests that PbO has taken some B_2O_3 in solid solution, since the conversion from Pb_3O_4 to PbO occurs at 560 ° C in the case of pure oxides. This means that the existence of PbO as solid solution has destabilized Pb_3O_4, causing its decomposition to PbO at a temperature much lower than in the case of pure oxides.

This phenomenon has been reported in other systems containing PbO (see e.g. ref. 24). On the ternary diagram this shows up as a series of tie lines joining Pb_3O_4 and PbO (s.s.) over the temperature range 490–560 ° C.

However, it has not been possible to determine whether the PbO solid solution contains a stoichiometric amount of O_2 or excess O_2. For this reason, the boundary of this solid solution has been shown dotted on the diagram.

In view of the present results, particularly the comparative analysis of X-ray results shown in Table 3, it would seem that the previously reported compounds $PbO \cdot B_2O_3$, $5PbO \cdot 4B_2O_3$ and $9PbO \cdot 8B_2O_3$ are members of the $PbO \cdot B_2O_3$ solid solution, containing excess PbO.

The quasi-binary temperature–composition diagram in air

To facilitate following up the various phase changes that occur as heating of mixtures of PbO_2 and B_2O_3 begins, the ternary isobar shown in Fig. 8 has been projected on the binary diagram shown in Fig. 11. We should note, however, that this diagram represents only the sequence of phases appearing on heating and their compositions. It is not a true binary diagram and hence the phase rule cannot be applied in this case.

On this diagram the stoichiometry of B_2O_3, $PbO \cdot B_2O_3$, $2PbO \cdot B_2O_3$ and PbO is apparent, as well as the various eutectoid situations associated with the decomposition of different phases. Melting behaviour was not investigated in the present study, so the liquidus data were taken from the work of

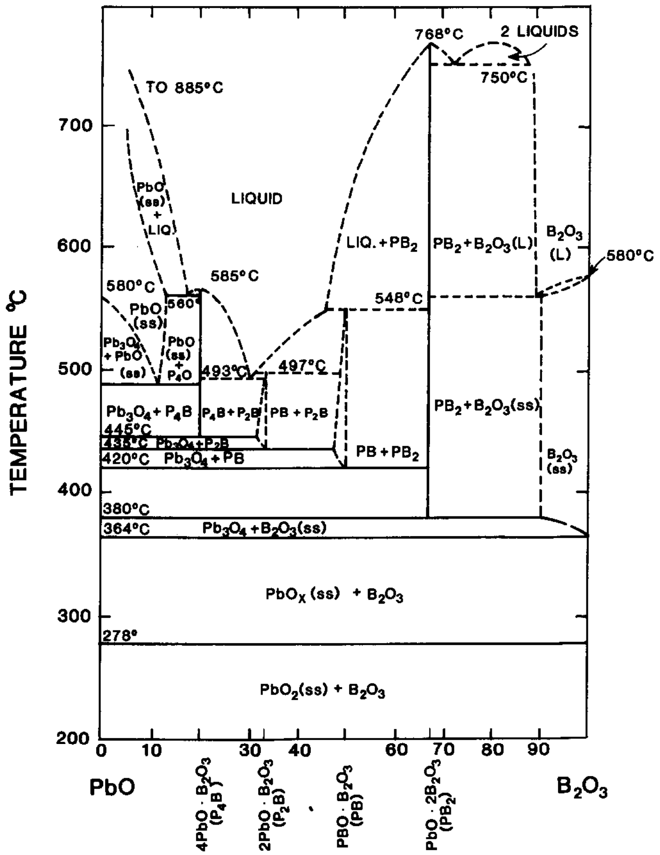

Fig. 11. Quasi-binary isobaric section for the system PbO_2–PbO–B_2O_3 in air.

Geller and Bunting [14] and Liedberg et al. [19]. As the melting behaviour of B_2O_3 (s.s.) has not been reported in previous works this has been shown tentatively on the diagram by fixing the melting point of pure B_2O_3 at about 580 °C [14] and assuming the presence of a eutectic point between B_2O_3 and PbO · $2B_2O_3$, deduced from the DTA curve in Fig. 4 where the endothermic peak corresponding to melting starts at 580 °C.

Also, on the projected binary the solidus and liquidus patterns at the monotectic point have been corrected in view of the previously explained criticism of the diagram of Geller and Bunting [14].

Finally it must be noted that allotropic transitions reported by several authors have not been included on this diagram (see Table 2).

CONCLUSIONS

From the isobaric section constructed for the system PbO_2–PbO–B_2O_3 we draw the following conclusions.

The previously reported compounds $PbO \cdot B_2O_3$ (PB), $5PbO \cdot 4B_2O_3$ (P_5B_4) and $9PbO \cdot 8B_2O_3$ (P_9B_8) are members of the $PbO \cdot B_2O_3$ solid solution, containing an excess of PbO.

The compounds $PbO \cdot 2B_2O_3$ (PB_2), $PbO \cdot B_2O_3$ (non-stoichiometric), $2PbO \cdot B_2O_3$ (P_2B) (non-stoichiometric) and $4PbO \cdot B_2O_3$ (P_4B) have been obtained and their stability regions fixed. It has also been found that PbO exists in this system as a solid solution.

Seven invariant situations at which three condensed phases and oxygen coexist in equilibrium were obtained on the ternary diagram:

(i) at about 278 °C B_2O_3, PbO_x ($x = 1.57$) and PbO (s.s.);

(ii) at 364 °C B_2O_3, PbO_x ($x = 1.41$) and Pb_3O_4;

(iii) at 380 °C B_2O_3 (s.s.), Pb_3O_4 and PB_2;

(iv) at 420 °C Pb_3O_4, PB_2 and PB (s.s.);

(v) at 435 °C PB (s.s.), P_2B (s.s.) and Pb_3O_4;

(vi) at 445 °C P_2B (s.s.), P_4B and Pb_3O_4;

(vii) at 490 °C P_4B, PbO (s.s.) and Pb_3O_4.

Five monovariant situations in which two solid phases and oxygen coexist in equilibrium were observed.

(a) At temperatures of 100–278 °C B_2O_3 coexists in equilibrium with PbO_2 (s.s.) and O_2.

(b) At temperatures of 278–364 °C PbO_x (s.s.) coexists in equilibrium with B_2O_3 and O_2.

(c) At temperatures of 364–380 °C B_2O_3 takes some Pb_3O_4 in solid solution and coexists in equilibrium with O_2.

(d) At temperatures of 420–435 °C PB (s.s.) coexists in equilibrium with Pb_3O_4 and O_2.

(e) At temperatures of 435–445 °C P_2B (s.s.) coexists in equilibrium with Pb_3O_4 and O_2.

It has not been possible to determine whether the PbO solid solution contains a stoichiometric amount of O_2 or excess O_2. The compounds in this system starting with PbO_2 as the original oxide were formed at equilibrium temperatures lower than the corresponding temperatures if PbO had been used as the starting material.

REFERENCES

1 I. Masuda, Hoya Corp., Japan-Kokai 7850, 217 (Cl. C03C3/04), 8 May 1978.
2 F.B. Gorden and J.K. Norbert, J. Am. Ceram. Soc., 35 (1952) 259.
3 E. Rykiert, J. Korowski and A. Swiatch, Szklo. Ceram., 35 (1984) 8.
4 B.S. Chiou, Inst. Elect. Natl. Chiaotung Univ., Taiwan (1984).
5 N.Y. Ermolenko, V.I. Shamkalovich and E.M. Dyatlova, Steklo Sitally Silik., 7 (1978) 12.
6 V.N. Fedrov, L.I. Panov, Ju. Kornatovski, E.V. Machonina and V.S. Dobroer, (USSR) Prom. Obraztsy Tovarnye Znaki, 37 (1983) 82.

7 Asahi Glass Co. Ltd., Japan-Kokai, Tokyo Koho Jpn. 57,140,340 (Cl. C03C17/04), 30 August 1982.
8 W.D. Rudowska, R. Debicki and A. Kostur, Polish Patent 98,328 (Cl. C2305/04), 15 December 1978.
9 Mitsubishi Elect. Corp., Japan-Kokai Tokyo Koho 81,26,747 (Cl. C03C3/30), 14 March 1981.
10 Nippon Elect. Glass Co. Ltd., Kokai-Tokyo Jpn. 58,161,942 (Cl. C03C3/12), 26 September 1983.
11 A. Van and J. Paul (Phillips), European Patent (Cl. C03C27/100), 27 May 1981.
12 M.V. Sergeeva, E. Mamchits, G. Martyneko, P. Miroshnikov and Yu. Goltsov, USSR Patent 785, 268 (Cl. C04B35/00), 7 December 1980.
13 H. Bauer and G. Plotcher, Z. Anorg. Allg. Chem., 350 (1967) 275.
14 R.F. Geller and E.N. Bunting, J. Res. Natl. Bur. Stand., 18 (1937) 585.
15 H.F. McMurdie, J. Res. Natl. Bur. Stand., 26 (1941) 489.
16 I.G. Mel'nikova, K.S. Evatropen and A. Kuzentsov, Zh. Fiz. Khim., 25 (1951) 1317.
17 V.T. Maltsev, P.M. Chobanyan and V.L. Volkov, Zh. Neorg. Khim., 19 (1974) 1917.
18 M.F. Abadir, A.M. Gadalla and J.M. Agamawi, Trans. J. Brit. Ceram. Soc., 75 (1976) 68.
19 D.Y. Liedberg, C.G. Ruderer and C.G. Bergeron, J. Am. Ceram. Soc., 48 (1965) 440.
20 X-ray card, No. 3-0533 (ASTM).
21 X-ray card, No. 3-0094 (ASTM).
22 B. Cullity, Elements of X-ray Diffraction, Addison Wesley, Reading, MA, 1956.
23 X-ray card, No. 3-0339 (ASTM).
24 S. Shaaban, M.F. Abadir and A.N. Mahdy, Trans. J. Brit. Ceram. Soc., 83 (1984) 102.